Table 4.4 Results for removal of copper in a packed bed cell

Dependence of Current Efficiency on Copper Concentration	
Flowrate : 1,93 l/min	Cell current : 4,0 amps
Specific conductivity : 14,03 mmho/cm	H_2SO_4 in catholyte : 1,0 g/l
Copper Concentration (ppm)	**Current Efficiency**
83,0	0,842
51,1	0,698
25,3	0,467
11,5	0,231
6,5	0,125

Dependence of Current Efficiency on Catholyte flowrate		
Average copper concentration : ~24ppm	Cell current : 4,0 amps	
Specific conductivity : 14,03mmho/cm	H_2SO_4 in catholyte : 1,0 g/l	
Flowrate (l/min)	**Copper Concentration(ppm)**	**Current Efficiency**
2,28	26,5	0,495
1,92	25,7	0,456
1,67	24,7	0,432
1,21	23,4	0,355
0,76	22,6	0,234
0,36	19,9	0,137

5. DISCUSSION

> 'This, along with standard deviations of 10 or 20 percent in the exchange-current-density values, indicates the electrode kinetics are, in general, neither predictable nor reproducible on solid electrodes'.

This quotation (63), from the work of one of the leading authorities on modern electrochemistry, aptly underlines the principal difficulty encountered in electrochemical research and design. The problem hinges on the fact that electrochemical kinetics describe surface phenomena and, while the basic theoretical results are well established, the precise value of the electrochemical kinetic parameters, and in particular the exchange current density, are critically dependent on the exact nature of the electrode surface. Surfaces can, and do, change even in the course of a single experiment or series of experiments and this fact should be borne in mind whenever the results of electrochemical kinetic investigations are discussed.

5.1 Determination of Electrochemical Kinetic Parameters using the Analytical Solution of the Porous Electrode Equation

The analytical solution to the porous electrode equation is given in Section 2.3. By means of simultaneous solution of this equation for a number of experimental conditions it is theoretically possible to calculate the values of the model parameters and to convert these into values of the electrochemical kinetic parameters.

This method proved to be unsuitable for application to the results of the experimental investigation of nickel removal from dilute solution, even though the required potential measurements were available. The extremely low conductivity of the solution phase produces a very large potential gradient at the free surface of the electrode, which means that any potential measurements at that interface are critically sensitive to the positioning of the measuring probe and are extremely sensitive to ohmic potential drop. In a very few cases there was also some evidence of the evolution of bubbles of hydrogen gas within the electrode. In that case the formation

of these bubbles leads to fluctuations in the local specific interfacial areas and hence in the local potentials and current densities.

As the potential terms appear as exponents in the analytical solution (equation [2.49]) such relatively small uncertainties in the potential measurements achieve quite considerable significance and serve to preclude any meaningful values of the kinetic parameters being obtained from the experimental results. The analytical approach was therefore abandoned and the experimental results are analysed using the numerical technique outlined earlier. This method still offers promise, however, in obtaining kinetic data for porous electrode systems having good solution conductivity and in which disturbances due to gas evolution are either absent or negligible.

5.2 Application of the Numerical Solution of the Porous Electrode Equation to the Results for Nickel Reduction

5.2.1 Introduction

The experiments on nickel reduction were characterised by the very low conductivity of the catholyte solution, particularly towards the end of each experimental run, and by large variations in the catholyte pH during the course of a run. The effect of migration, as outlined in section 2.1.5, has therefore been taken into account in fitting the mathematical model to the experimental results (see Appendix C). Consideration has also been given to the effects of pH on the electrochemical kinetic parameters.

For the purposes of fitting the model the short induction period which was observed at the start of each experimental run, during which current efficiencies and electrode potentials rose rapidly to normal operating values, was ignored. Such induction periods have been observed in other work on packed bed electrodes (21,28) and have been ascribed to the reduction of oxide layers which may have built up on the bed surface during offline periods.

It should therefore be possible to establish the validity of the assumption of negligible limitation on the side reaction rate by calculating the local current density profiles through the packed bed electrode and confirming whether or not the local current density has reached levels where side reaction limitations may be significant.

Available kinetic data (Appendix G) indicate that the cathodic transfer coefficients for both nickel reduction and hydrogen evolution are approximately 0,5. The initial attempts at fitting the experimental results therefore concentrated on finding best values for the kinetic parameters k_1 and k_2, with the beta values of both main and side reactions set equal to one another at

$$\beta_1 = \beta_2 = -\frac{0,5F}{RT} = -19,5 \text{ volts}^{-1} \qquad [5.1]$$

This search for the best values of the two parameters was performed using a programmed version of Powells method (79) to minimise an objective function which was taken to be the sum of squared errors between experimentally measured current efficiencies and values of the current efficiencies calculated by the mathematical model. Poor fits were obtained. The minimum value of the objective function in this case was found to lie on a line with an equation

$$\log k_2 = \log k_1 + \text{const} \qquad [5.2]$$

which echoes the relationship between the parameters implied in equations [2.36] and [2.37]. As it soon became obvious that a reasonable fit to the experimental results could not be obtained by simply finding suitable values of k_1 and k_2 at these beta values this approach was abandoned in favour of an alternative line of attack which yielded far better results.

5.2.2 Fit of the Model to the Experimental Results

As it was anticipated that the electrochemical kinetic parameters might be influenced by the catholyte pH, separate sets of data at pH4, pH5, pH6, pH7 and pH8 were extracted from the results given in Appendix A. Each set of data was then the subject of an independent fit.

5.2.2.1. Fits with Conventional Hydrogen Evolution Reaction Electrochemical Kinetic Parameters

An initial assumption was made that the side reaction consisted only of the process of hydrogen evolution and could be described by Tafel kinetics based on literature values of the electrochemical kinetic parameters for the hydrogen evolution reaction on nickel. It was also assumed that the particular form of the porous electrode equation given in equation [2.34], which assumes negligible mass transfer limitation on the side reaction, is applicable.

Some early workers have reported apparent limiting current densities for hydrogen evolution on nickel at cathodic current densities greater than 10^{-2}A/cm^2 (138-140), but these effects have subsequently been explained as resulting from incorrectly compensated ohmic potential drops and impurities in solution (66, 141, 142). Straight line Tafel slopes for hydrogen evolution on nickel have been measured by many workers at current densities of up to 1,0 A/cm^2 in acid and alkaline solutions (143-146), although at current densities greater than 1,0 A/cm^2 the experimental current density begins to deviate from the Tafel form and eventually appears to reach a saturation value of around 10^2 A/cm^2 at very negative over-potentials (147). In the latter case the authors conclude that the limitation does not arise as the result of mass transfer limitations on the rate of transport of reactive species to the electrode, but rather as the result of complete coverage of the electrode surface by adsorbed hydrogen atoms, with the rate of recombination of adsorbed hydrogen atoms into H_2 molecules constituting the rate determining step of the hydrogen evolution reaction.

5.2.2.2 Fits with a General Side Reaction

When it became apparent that application of literature values of the kinetic parameters of the hydrogen evolution reaction to the side reaction incorporated in the mathematical model equations resulted in a very poor fit of the experimental results, it was decided instead to fix both parameters k_1 and β_1 for the main reaction and to obtain experimentally fitted values of k_2 and β_2 for a general side reaction.

The electrochemical kinetic data for the nickel reduction reaction plotted in Figure G.1 are so widely scattered as to effectively mask the possible systematic variation in the values of the parameters over the pH range of significance to the present investigation. Values of

$$i_{o,Ni}\ (1,0M,\ 25^{o}C) = 1 \times 10^{-5}\ A/cm^{2}$$

and $\alpha_{c,Ni} = 0,59$

were therefore chosen by inspection of the plotted data and taken to apply over the entire pH range covered in this investigation.

With the kinetic parameters for the main reaction now defined it should be possible to fit the experimental data by a suitable choice of the values of the parameters for the side reaction.

Figure 5.1 shows a contour plot of the variation with k_2 and β_2 of the objective function for the fitting of a representitive sample of the experimental data at pH6. Similar plots are obtained for data at the other pH values. The figure shows a definite minimum in the value of the sum of squared errors objecti.e functions in the area around

$$k_2 = -1 \times 10^{-4}\ A/cm^{2}$$

$$\beta_2 = -4,0\ volts^{-1}$$

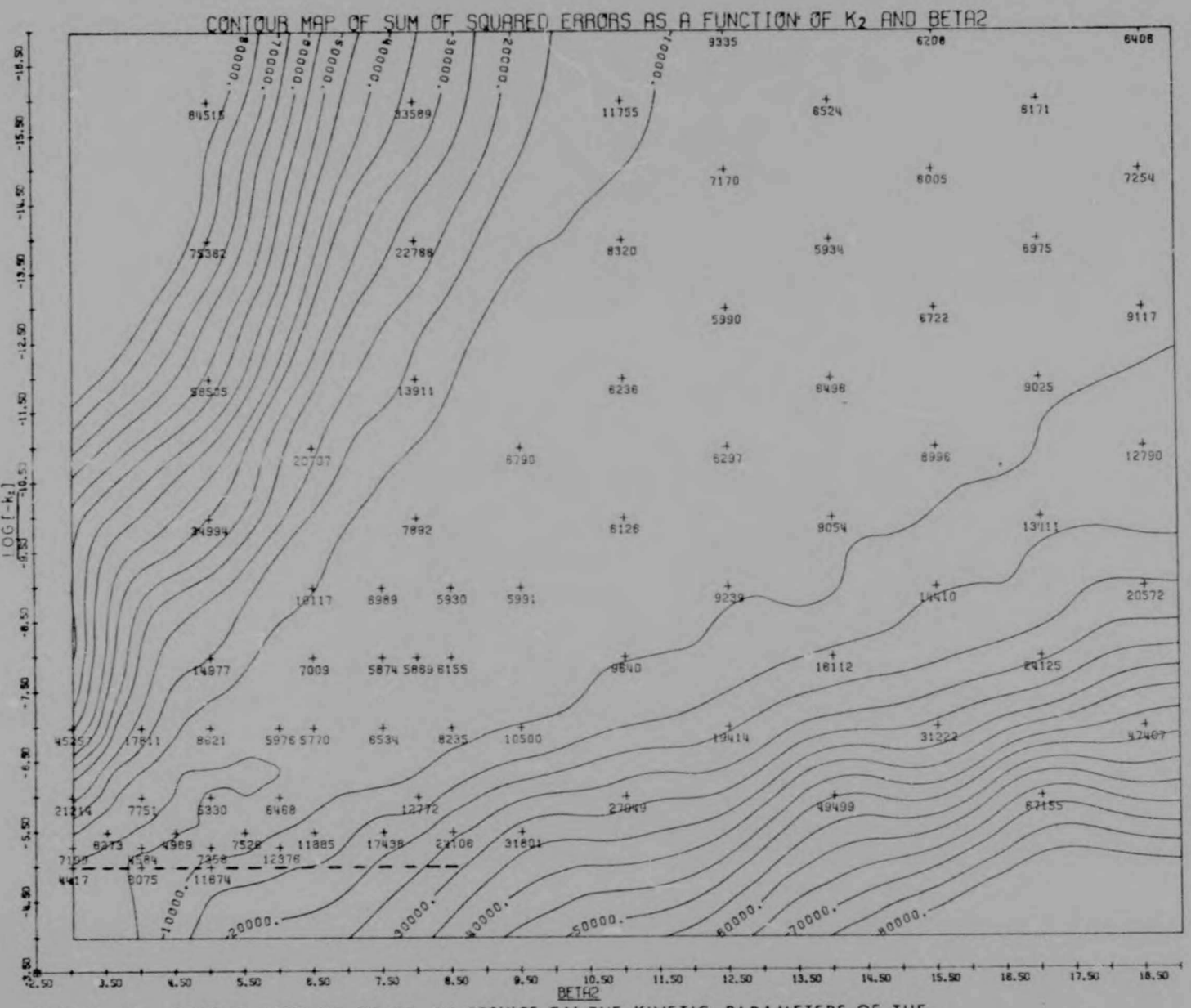

FIGURE 5.1 . DEPENDANCE OF FIT OF Ni RESULTS ON THE KINETIC PARAMETERS OF THE SIDE REACTION.

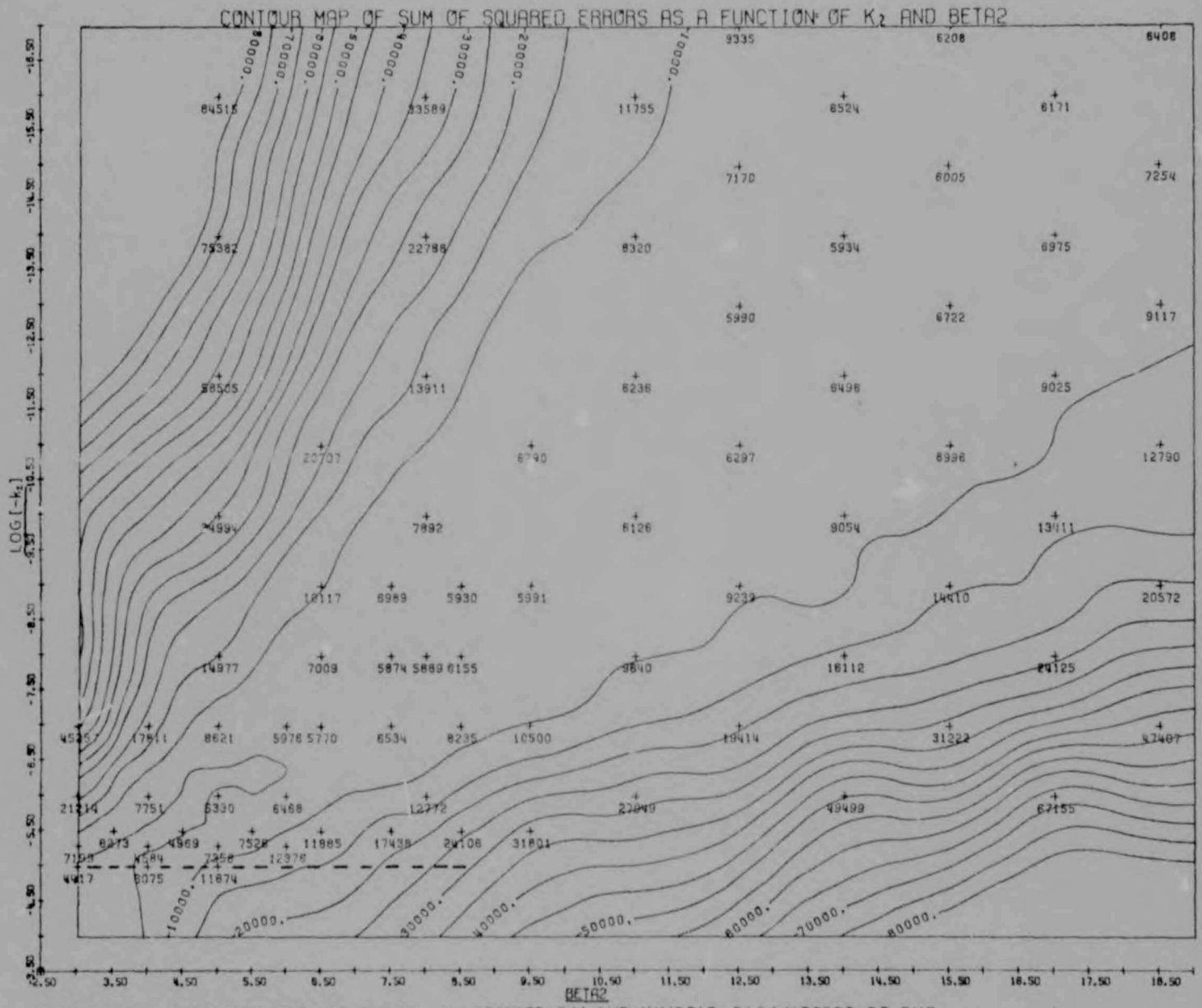

FIGURE 5.1 . DEPENDANCE OF FIT OF Ni RESULTS ON THE KINETIC PARAMETERS OF THE SIDE REACTION.

The β_2 value corresponds to a transfer coefficient for the side reaction of approximately $\alpha_{c,S} = 0,1$ and a cathodic Tafel slope of 575 millivolts per decade. This Tafel slope is far removed from the value of 120 millivolts normally obtained for hydrogen evolution on nickel, but is in good general agreement with the later results obtained in independent experiments at the rotating disc electrode.

Other features of the contour plot are the high values obtained for the objective function under conditions of small β_2 values combined with small k_2 values, and under conditions of relatively large β_2 values combined with large k_2 values.

The first situation corresponds to very high values of the calculated current efficiency ($\xi_{Ni} \approx 1,0$) and the second to very low values ($\xi_{Ni} \approx 0$). There is also a broad region between the two extremes where poor to mediocre fits are obtained. This region includes the β_2 values of -19,5 $volts^{-1}$ for which the poor fits discussed earlier were obtained.

At absolute values of k_2 much greater than 10^{-4} the model begins attempting to predict anodic potentials in parts of the electrode close to the current feeder. This is contrary to both the experimental observations and the assumptions used in deriving the model equations. A value of $|k_2| = 1 \times 10^{-4}$ A/cm^2 may therefore be taken as representing the upper bound for this parameter and this is indicated by a broken line in Figure 5.1.

The value of β_2 may be expected to be fairly insensitive to changes in pH. On the other hand, no explicit concentration dependence for the exchange current density is incorporated in the mathematical model and k_2 might therefore display some pH dependence. This possibility was explored in a new fit of the experimental data which is based on the relationships between the kinetic parameters depicted in Figure 5.1.

Once again k_1 and β_1 were kept constant and the value of β_2 was now also fixed at the value of $\beta_2 = -4,0$ $volts^{-1}$ which is indicated in Figure 5.1 as being a suitable choice for producing a reasonable fit of the experimental results.

The best fits of the experimental data at the various pH values may then be determined by a correct choice of k_2, the last remaining kinetic parameter. The results of this fit are shown in Figures 5.2 to 5.6 which give a comparison of the experimentally measured current efficiency values with the theoretical predictions of the mathematical model. Further details of the actual numerical values are given in Tables H1 to H5 of Appendix H. The variation of the fitted value of k_2 with pH is shown in Figure 5.7.

5.2.3 Discussion

5.2.3.1 General Observations

The entire range of experimental conditions detailed in Table 4.1 is represented in the data points of Figures 5.2 - 5.6. A good fit was obtained, particularly in the light of Newman's remarks quoted at the start of this chapter.

A striking feature of all the plots is that for large values of the experimental current efficiency the data points tend to lie on the high side of the $\xi_{measured} = \xi_{calculated}$ line. As the efficiencies decrease the calculated values tend first to coincide with the experimental results and ultimately, at very low current efficiencies, become smaller than the experimental values. This behaviour is probably the result of anisotropy in the relatively thin packed bed electrodes used in the study.

The mathematical model assumes that the surface area per unit volume is uniform across the entire thickness of the electrode and any wall effect is thus neglected. With a bed thickness/particle diameter ratio of 1,72 however, wall effects are far from negligible and an uneven specific surface area distribution will result. The actual specific surface area will be greatest in the centre of the electrode and will have a smaller value at the edges. The effect of bed anisotropy is therefore to give an unfair weighting to the calculated values of the partial currents close to the free solution interface, as the current densities in that region should, strictly speaking, be multiplied by a lower specific surface area factor than applies towards the centre of the bed.

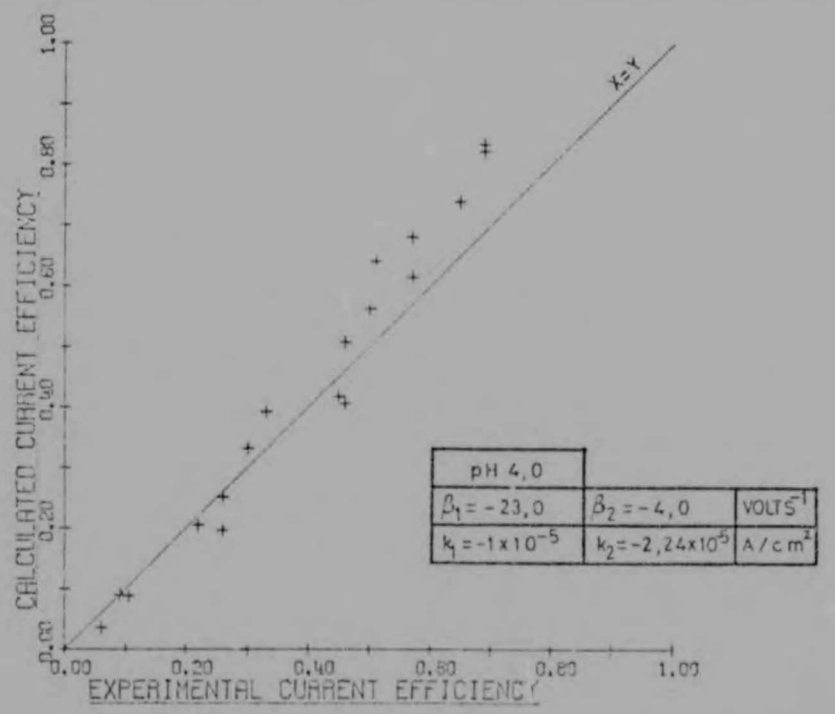

FIGURE 5.2 . FIT OF MODEL TO NICKEL RESULTS AT pH4 .

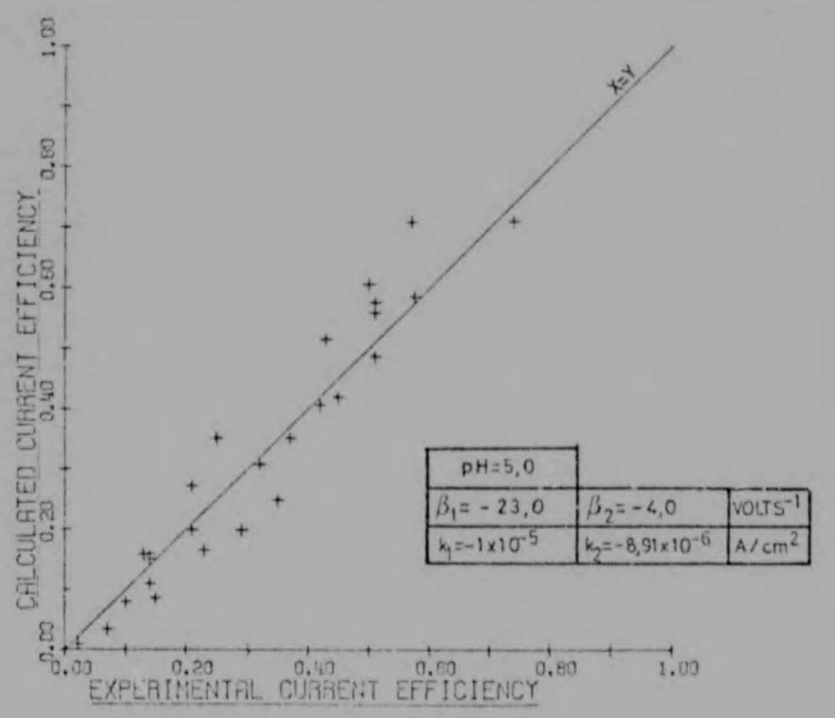

FIGURE 5.3 . FIT OF MODEL TO NICKEL RESULTS AT pH5 .

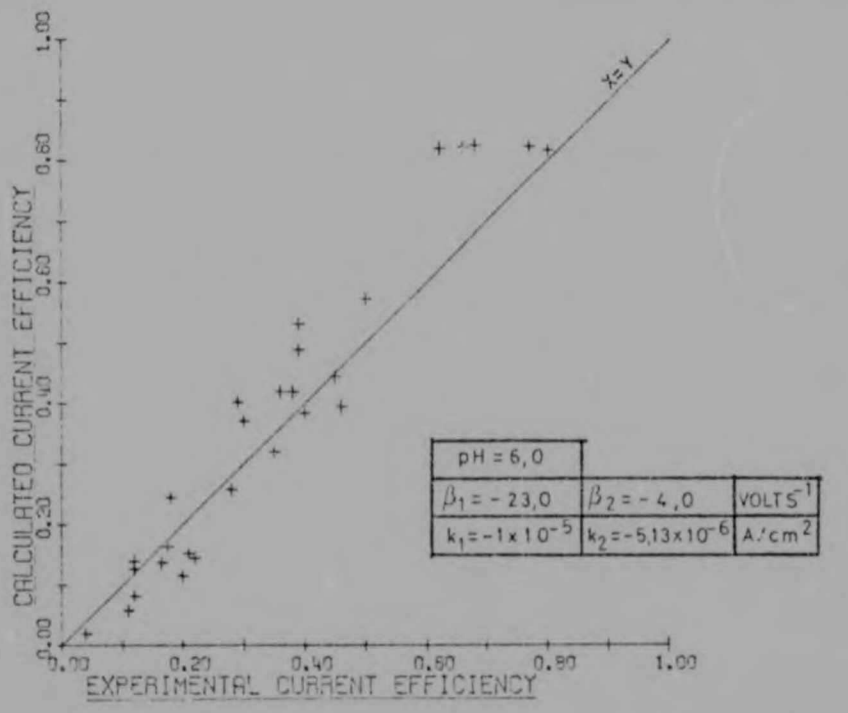

FIGURE 5.4 . FIT OF MODEL TO NICKEL RESULTS AT pH6 .

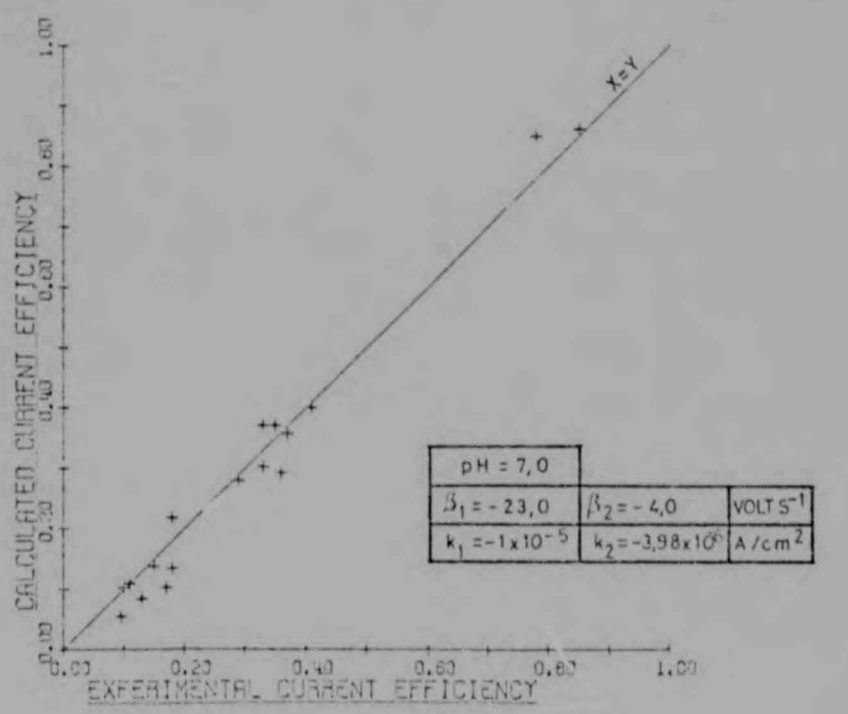

FIGURE 5.5 . FIT OF MODEL TO NICKEL RESULTS AT pH 7 .

FIGURE 5.6 . FIT OF MODEL TO NICKEL RESULTS AT pH8 .

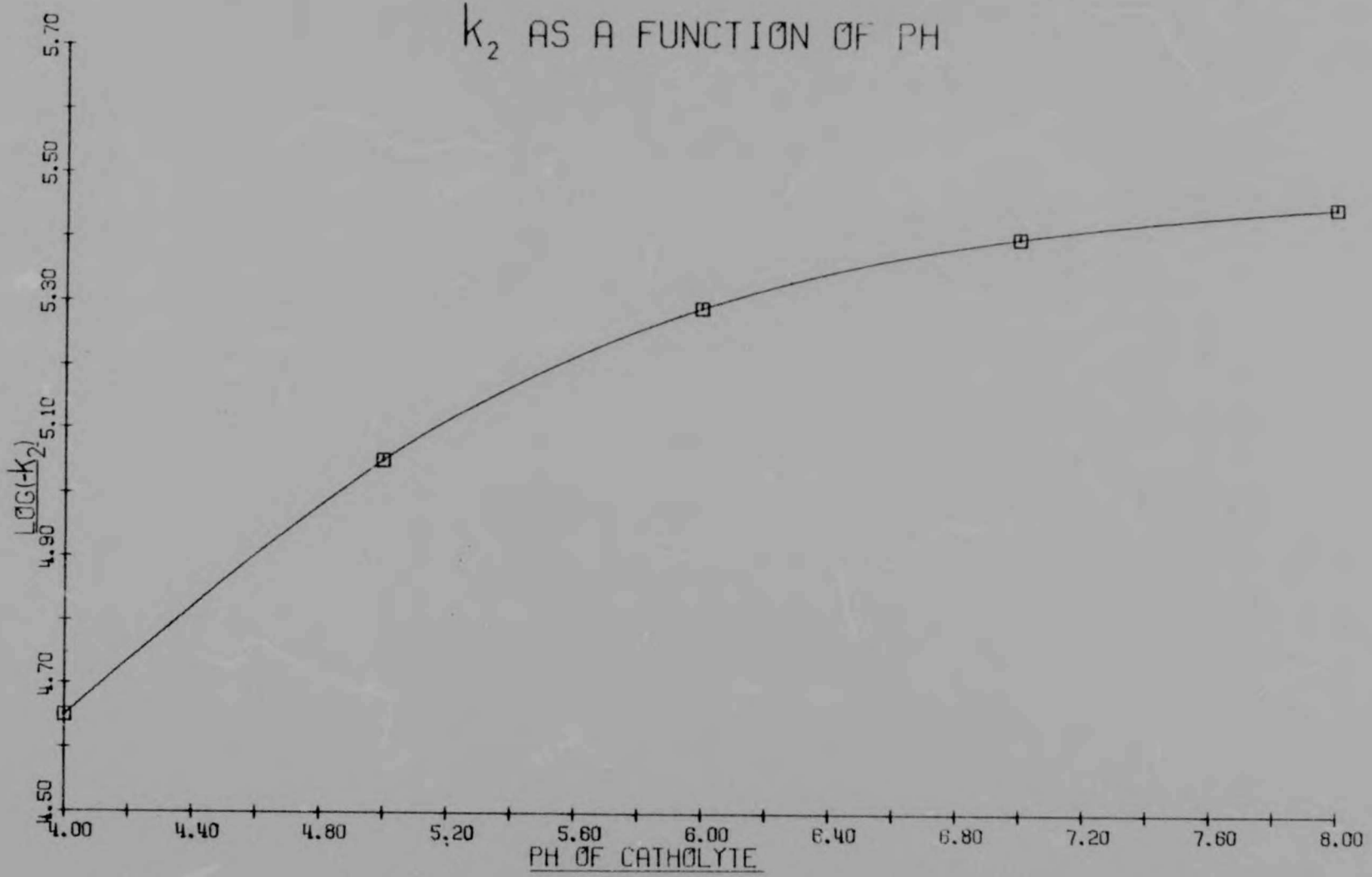

FIGURE 5.7. pH DEPENDANCE OF THE k_2 VALUES GIVING THE BEST FITS OF THE NICKEL RESULTS

As most of the electrochemical reaction tends to take place in the region of the free solution interface the current efficiency calculated in this region has a major influence on the overall current efficiency of the electrode. Therefore, when the model predicts a high current efficiency at the free solution interface too much emphasis is placed on this fact and an overall current efficiency which is too high results. On the other hand, too great a significance is also attached to very low current efficiencies calculated at the interface and these result in calculated overall values which are lower than they should be.

Values of the calculated electrode currents are compared with the actual experimental values in Appendix H. In all cases the calculated value is slightly too high as a consequence of the approximate method of numerical integration used in obtaining the values. The difference between calculated and experimental current values is, however, hardly significant, since the difference is less than one per cent in all cases.

Certain higher order terms of the Taylor series expansion of the partial current density function are discarded in the course of the mathematical derivation of the equations for the numerical solution to the packed bed electrode equation (Appendix B). The validity of this assumption was confirmed for all the experimental data points used in fitting the mathematical model : in all cases the last term retained in the solution was found to be at least 400 times as large as the first discarded term (for $\varepsilon_1 = 0,05$).

5.2.3.2 Val f the Kinetic Parameters

In the fitti of the experimental results for nickel removal the electrochemical kinetic parameters for the nickel deposition reaction are fixed at the best values obtained from a search of the available literature. The current efficiency results are then fitted by choosing appropriate values for the exchange current density and Tafel slope for the side reaction. A Tafel slope of 575 millivolts proved suitable at all pH values in the range pH 4 - 8, whereas k_2 is a function of pH and varied from $-2,25 \times 10^{-5}$ amperes per square centimetre at pH4 to $-3,55 \times 10^{-6}$ amperes per square centimetre at pH8.

The value of the parameter k_2 has been defined by the equation

$$k_2 = -i_{o\,S,ref.}\, e^{-\beta_2 \Delta U} \qquad [2.37]$$

where $$\Delta U = U_S - U_R \qquad [B.19]$$

Under the reference conditions chosen for the principal and secondary reactions ($[Ni^{2+}] = [H^+] = 1$ mole/l, $p(H_2) = 1$ atm, 25^oC) the value of ΔU is

$$\Delta U = 0{,}000 - (-0{,}23) = 0{,}23 \text{ volts}$$

and hence

$$e^{-\beta_2 \Delta U} = \exp\,(\,4{,}00 \text{ volts}^{-1} \times 0{,}23 \text{ volts}) = 2.51$$

Values of the fitted exchange current densities for the side reaction calculated from equation 2.37 , given in Table 5.1, exhibit a very weak dependence on the hydrogen ion concentration.

Table 5.1 Fitted values of the exchange current density for the side reaction during nickel deposition

pH	k_2 (A/cm^2)	$-i_{oS,\,ref.}$ (A/cm^2)
4	$-22{,}4 \times 10^{-6}$	$-8{,}93 \times 10^{-6}$
5	$-8{,}91 \times 10^{-6}$	$-3{,}44 \times 10^{-6}$
6	$-5{,}13 \times 10^{-6}$	$-2{,}04 \times 10^{-6}$
7	$-3{,}98 \times 10^{-6}$	$-1{,}59 \times 10^{-6}$
8	$-3{,}55 \times 10^{-6}$	$-1{,}41 \times 10^{-6}$

In considering the fitted experimental values of the electrochemical kinetic parameters for the side reaction it is therefore necessary to account for:

(a) A value for the Tafel slope considerably different to the literature value for hydrogen evolution on nickel, and
(b) The experimental pH dependence of the exchange current density for the side reaction.

In considering the first aspect it is well known that large numerical values of Tafel slope have been reported for hydrogen evolution on non-metals (12) and at metallic oxides and semiconductors (66, 77, 87, 88, 149-151). It is known that the kinetics of electrochemical reactions at semiconducting electrodes differ considerably from those at metal electrodes, chiefly as a result of limitations on the movement of electrons or holes within the semi-conducting material itself. Despite these differences the electrochemical kinetics of semi-conductor materials are however, still governed by Tafel-type equations and these equations do allow for very much larger numerical values of the Tafel slope than does the conventional equation for metal electrodes (87).

Since both NiO (152-154) and $Ni(OH)_2$ (86) have semiconducting properties there exists the possibility of hydrogen evolution at such a non-metallic surface with a large numerical value of the cathodic Tafel slope.

A NiO surface oxide exists on all nickel surfaces which have been handled in air, no matter what surface preparation stages have previously taken place (154). This oxide is readily reduced by steady state cathodic polarisation in acid and alkaline solution (145, 152, 153, 155). The surface oxide formed by anodic oxidation of nickel is, however, removed far less readily in acid solution of pH $\leq$ 2,8 and is not entirely reduced in less acidic solutions (152,153,155), even after extensive cathodic polarisation which is accompanied by an increase of up to 250% in the rate of hydrogen evolution (152).

Precipitation of nickel hydroxide from the bulk of the flowing catholyte is unlikely. The equilibrium curve (81-83) for the $Ni^{2+}/Ni(OH)_2$ system in Figure 5.8 indicates that no significant precipitation of nickel hydroxide from the solutions used in this investigation is possible below pH7,4. Since pH values greater than 7,5 were generally only reached towards the end of the experimental runs, when the nickel concentrations had already reached quite small values, precipitation is not very likely even under more alkaline conditions. Precipitation of nickel hydroxide at the surface or within the diffusion layer is nevertheless a distinct possibility.

The overall hydrogen evolution reactions in acidic or neutral solution

$$2H^+ + 2e \rightleftharpoons H_2 \qquad \text{(acid solution)} \qquad [5.3]$$

$$\text{or} \quad H_2O + 2e \rightleftharpoons H_2 + (OH)^- \qquad \text{(neutral solution)} \qquad [5.4]$$

either consume hydrogen ions or generate hydroxyl ions. As there exists a finite rate of diffusion of hydrogen ions into the boundary layer and a finite rate of diffusion of excess hydroxyl ions out of this layer, a certain degree of alkalisation of the boundary layer must take place. The actual extent of the alkalisation depends on a number of factors which include the current density, boundary layer thickness and the magnitudes of the diffusion coefficients.

Under certain conditions the pH within the boundary layer can rise to quite high values. Typical surface pH measurements of 7,5-8(84) and up to 9,5 (83) have been reported for solutions having a bulk pH of 5 or less. At such alkaline pH values the equilibrium for the reaction

$$Ni^{2+} + 2OH^- \rightleftharpoons Ni(OH)_2 \qquad [5.5]$$

is driven well over to the right hand side and significant quantities of nickel hydroxide can form on the electrode surface (81, 85). The rate of formation of such layers has been investigated and has been found to depend on a critical current density (81), below which no hydroxide precipitation can take place.

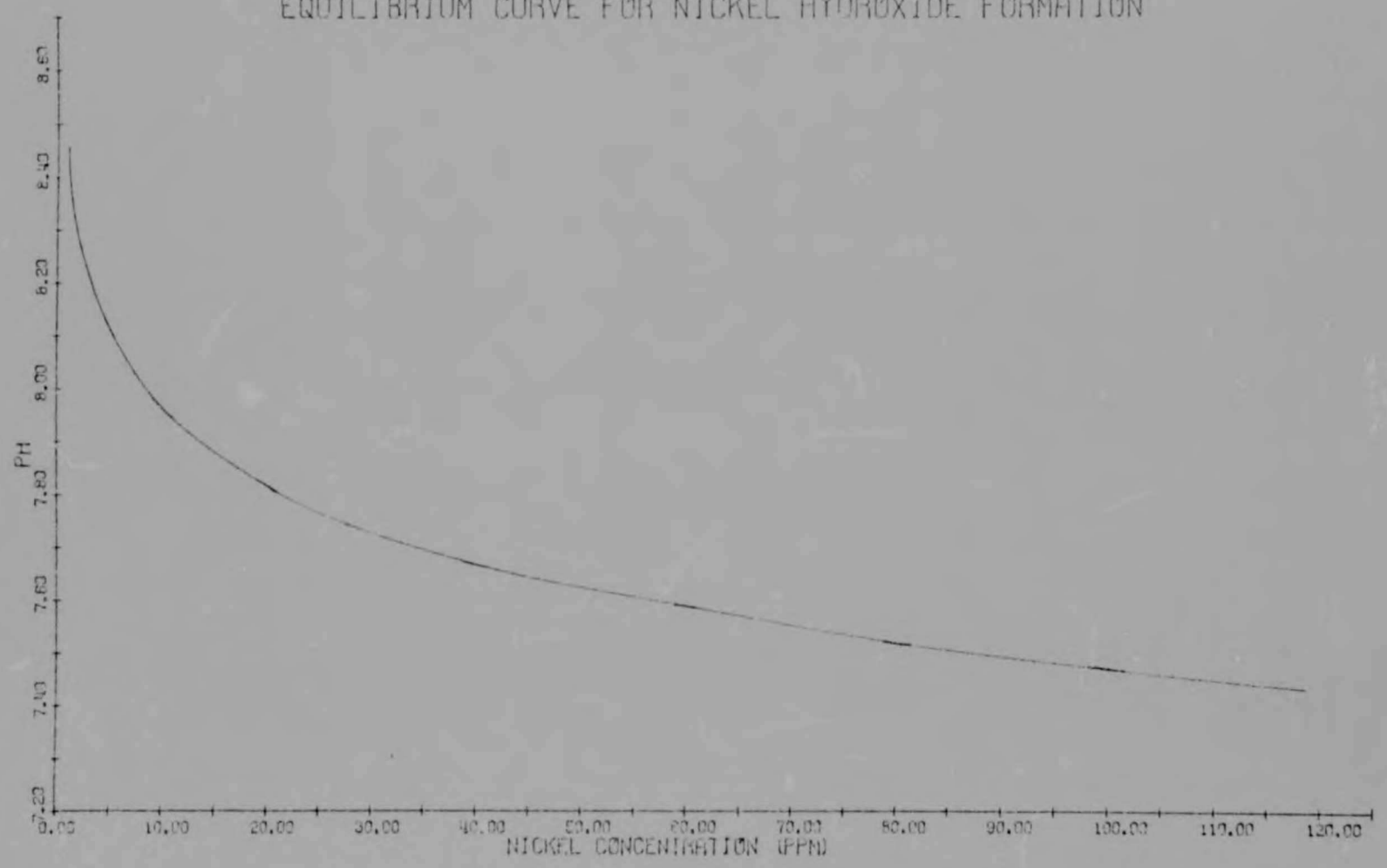

FIGURE 5.8. EQUILIBRIUM CURVE FOR NICKEL HYDROXIDE FORMATION.

During hydrogen evolution at an hydroxide surface the hydroxide itself could be reduced according to the reaction

$$Ni(OH)_2 + 2e \rightleftharpoons Ni + 2OH^- \qquad [5.6]$$

the existence of which has been experimentally confirmed (89). Other experimental results (83, 81) indicate however that once the hydroxide is formed all further reduction of nickel ceases and the hydrogen evolution reaction, accompanied by further deposition of nickel hydroxide, takes over completely, with the net electrochemical reaction being given by

$$Ni^{2+} + 2H_2O + 2e \rightleftharpoons H_2 + Ni(OH)_2 \qquad [5.7]$$

It should also be noted that high numerical values of the Tafel slope for hydrogen evolution on nickel have been ascribed to poisons (140, 156) and to other impurities in solution (141). Concentrations of as little as 10^{-10} moles per litre of various impurities had a significant effect on the rate of hydrogen evolution and up to five-fold changes in Tafel slope were observed at very low concentrations of impurities.

In the foregoing discussion a number of processes have been mentioned which result in larger than normal values of the cathodic Tafel slope at nickel electrodes. The results of the main experimental investigation of nickel removal do not themselves provide any specific indication as to which, if any, of these processes might be responsible for the high numerical value of the fitted kinetic parameter for the side reaction, or whether the fitted value results from a deficiency in the mathematical model. In particular, since the results of the investigation are intended to be applicable to industrial situations, no particular effort was made to obtain ultrapure solutions. Although a reasonable degree of solution purity was established, there is nevertheless a distinct possibility that impurities could have been present in solution at concentrations considerably greater than the 10^{-10} moles per litre mentioned earlier, and that such impurities might significantly influence the electrochemical kinetics of the system.

The weight of evidence does, however, point more to an impurity effect than to surface oxide or hydroxide effects. As has already been mentioned the oxide produced in air is readily reducible at low cathodic overpotentials and the existence of a permanent surface layer of this oxide under the potential conditions encountered in this investigation is thus highly unlikely. Although the anodically produced oxide is far more resistant to cathodic reduction, the experimentally determined slope for the hydrogen evolution reaction at this oxide is even steeper than for the reaction at bare nickel (80mV versus 120-130mV)(153, 157). It is also unlikely that the kinetics of reactions [5.5]to [5.7] would be adequately described by the type of equation used successfully in the mathematical model and significant quantities of nickel hydroxide were, in any event, neither detected in the flowing electrolyte nor observed at the electrode surface during the course of the experimental runs.

The secondary investigation at a nickel rotating disc electrode described in Appendix D serves to clarify this point. Similar methods of solution preparation and de-aeration were used in order to make the rotating disc kinetic determinations comparable with the results of the main experimental program. The following conclusions may be drawn from the experimental results:

(a) Tafel-type kinetics are observed for the cathodic reaction at the nickel electrode in acidic and neutral solutions over a wide range of cathodic electrode potentials, pH, electrode speed and potentiodynamic sweep rate.

(b) The experimentally determined value of the apparent Tafel slope varies from 320-700mV and therefore brackets the value of 575mV fitted to the packed bed experimental results.

(c) Negative deviations from straight line kinetics at high current densities are predominantly due to uncompensated ohmic potential drop in the electrolyte.

(d) The value of the apparent Tafel slope is strongly dependent on the degree of aeration of the solution.

On the basis of the rotating disc electrode results it may therefore be concluded that the process of oxygen reduction is involved in the nett side reaction, which cannot simply be considered to be the hydrogen evolution reaction.

In the main experimental program the presence of oxygen in solution resulted from a contribution by the commercial nitrogen gas bubbled through the catholyte and used to blanket the top of the cell, together with contributions from diffusion through openings in the apparatus and through the plastic tubing of the electrolyte recirculation system. Similar effects have been observed by other authors (141), who conclude that, even with the most careful techniques of purification, the concentration of oxygen in systems without water sealed joints and taps can be reduced only to around 10^{-4} moles per litre. This represents a concentration of a similar order to the concentration of the principal reactant and a number of orders of magnitude greater than the hydrogen ion concentration prevailing during many of the experimental runs.

The overall nett side reaction is therefore extremely complex, comprising as it does contributions from each of the following reactions in acid and neutral solution.

$$2H^+ + 2e \rightleftharpoons H_2 \qquad [5.3]$$

$$O_2 + 2H^+ + 2e \rightleftharpoons H_2O_2 \qquad [2.33a]$$

$$H_2O_2 + 2H^+ + 2e \rightleftharpoons 2H_2O \qquad [2.33b]$$

The observed electrochemical kinetics of the reactions [2.33] contain both charge-transfer and diffusion components (66), and hence a complete description of the nett side reaction would require the replacement of a single term involving two electrochemical kinetic parameters (k_2 and β_2) in the simplified porous electrode equation [2.34] by at least three terms containing a total of six kinetic parameters plus assorted concentration dependencies.

In view of the many uncertainties still prevailing as regards the mechanism and kinetics of the oxygen reduction reaction, the incorporation of a large number of additional variables into an engineering model would undoubtably lead to results of rather dubious validity, although the fit of a model with four extra parameters would naturally appear to be rather better than the fit of a more simple model.

The results reported in Appendix D and in the literature by other workers (141, 158) indicate that under certain circumstances the combined processes of hydrogen ion and oxygen reduction may be lumped together in a single effective reaction which may be adequately described over a wide potential range by Psuedo-Tafel kinetics, based on a flatter apparent Tafel slope than is generally observed for simple electrode processes. Such an approach, when applied to the experimental results for nickel removal, leads to an average absolute error of 5,2% in the calculated percentage current efficiency for nickel removal, a quite acceptable accuracy for engineering calculations.

As mass-transfer and concentration effects are now also lumped into the effective kinetic expression for the overall side reaction the values of the apparent Tafel slopes are only directly comparible for different systems under similar hydrodynamic conditions. This condition is satisfied for comparison of the rotating disc electrode results with those of the packed bed electrode, as may be seen in Table 5.2 which summarises the results of the calculations detailed in Appendix J.

Table 5.2 Hydrodynamic similarity between rotating disc electrode and packed bed electrode

	Values of $D^{1}/_{3}/\delta$ for the experimental conditions of Appendix A & Appendix D	
	Minimum	Maximum
Packed bed electrode	9,0	27,1
Rotating disc electrode	9,4	26,6

The rotating disc electrode experiments did not demonstrate any clear dependence of the electrochemical kinetic parameters for the overall side reaction on the speed of rotation. However, as two of the processes lumped into the overall reaction are subject to mass transfer influences some variations must be expected to occur, particularly in the value of the apparent exchange current

density, and these minor variations may be expected to contribute significantly to the scatter observed in the model fits of Figures 5.2 to 5.6. Gross variations in the concentration of dissolved oxygen participating in the overall side reaction in the packed bed electrode were most unlikely, as the experimental conditions, especially with regard to the rate at which the commercial grade nitrogen was bubbled through the circulating catholyte, were standardised throughout the program of experimental runs. Minor concentration differences could however also have contributed to the scatter in the fitted results.

The observed pH dependence of the exchange current density for the side reaction may be qualitatively explained in terms of the electrochemical reaction orders of the various components of the overall side reaction. Experimentally confirmed values of the reaction orders with respect to the hydrogen ion are given in Table 5.3 (66), from which the anticipated pH dependence of $-i_{oS,\,ref}$ may be deduced from the result (66).

$$\frac{\partial \log \left| -i_{oS,\,ref} \right|}{\partial \log C_{H^+}} = \frac{\partial \log \left| -i_{oS,\,ref} \right|}{\partial\, pH} = z_{o,H^+} \qquad [5.8]$$

Table 5.3. Electrochemical reaction orders for side reaction processes

Reaction	$z_{o,\,H^+}$	
	Acid and Neutral Solution	Alkaline Solution
[5.3] $2H^+ + 2e \rightleftharpoons H_2$	1	-
[5.4] $H_2O + 2e \rightleftharpoons H_2 + (OH)^-$	-	0
[2.33a] $O_2 + 2H^+ + 2e \rightleftharpoons H_2O_2$	0	1
[2.33b] $H_2O_2 + 2H^+ + 2e \rightleftharpoons 2H_2O$	0	0

Equation [5.8] therefore predicts a linear pH dependence for $\log \left| -i_{oS,\,ref} \right|$ in acid and neutral solution and no dependence in alkaline solution, provided that it is assumed that the

hydrogen evolution reaction predominates in the overall side reaction. This prediction is consistent with the experimental results, which indicate a pH dependence of $-i_{oS,\,ref}$ under acidic conditions which becomes steadily weaker as the bulk catholyte becomes more alkaline, until around pH 8,0 the value is essentially independent of pH. Since some alkalisation of the hydrodynamic boundary layer at higher current densities will inevitably occur, thus leading to an effective pH at the electrode surface which is greater than that of the bulk solution, this observation is consistent with available information which indicates that the transition between reaction [5.3] and reaction [5.4]takes place around local pH 8 (66).

5.2.4 Further Predictions of the Mathematical Model for the Nickel Case

The fitted values of the electrochemical kinetic parameters for the main and side reactions have been used in producing plots of the overpotential, current efficiency and current density profiles across the packed bed electrode of the cell used in this investigation. The dependence of the profiles on nickel concentration, electrode current, catholyte flowrate and catholyte pH have all been investigated and the results are given in the following subsections. Results are also given for the overall electrode current efficiency under varying operating conditions. A set of 'core' conditions (50 ppm Ni, 5A, 3,0 l/min and pH6) are incorporated in each set of results in order to facilitate comparison.

The dimensionless length $X = {}^{x}/_{L}$ is used as the length scale for the various profiles. The potential profiles are for the local overpotential η, defined in Appendix B by the equation

$$\eta = \phi_1 - \phi_2 \qquad [B.20]$$

and which appears in the following expressions for the partial current densities of the main and side reactions